ADVANCED OPTICAL MATERIALS
www.advopticalmat.de

Single-Photon Emission from Single Microplate $MAPbI_3$ Nanocrystals with Ultranarrow Photoluminescence Linewidths and Exciton Fine Structures

Junyang Yuan, Dawei Zhou, Chen Zhuang, Yong Zhou, Chunfeng Zhang, Lin Wang, Min Xiao,* and Xiaoyong Wang**

Stimulated by the superior performance of organic–inorganic $MAPbI_3$ perovskite films in photovoltaic devices, a lot of research interest is now being devoted to their low-dimensional nanocrystals (NCs) to extend the optoelectronic functionalities as well as to promote the potential applications in quantum information technologies. Compared to other organic–inorganic and all-inorganic counterparts that have been intensively studied, the $MAPbI_3$ NCs suffer from the optical and chemical instabilities so that their single-particle photophysical properties have been largely unexplored up to now. Here, the authors have synthesized single $MAPbI_3$ microplates from a two-step method and characterize their optical properties mainly at the cryogenic temperature, showing that localized optical emitters are universally present with the quantum feature of single-photon emission. Photoluminescence (PL) linewidth measured for such a single quantum emitter can be as narrow as ≈200 µeV, as a direct consequence of its embedment inside the microplate with the spectral diffusion effect being greatly suppressed. This has allowed them to resolve the exciton fine structures from some of the studied single quantum emitters, each of which is manifested as a PL doublet with the energy separation of ≈600 µeV and the orthogonally linear polarizations.

1. Introduction

Encouraged by the superior performance of organic-inorganic perovskite films in solar cells and light-emitting diodes,[1–3] a lot of research attention has been recently devoted to the synthesis and characterization of their low-dimensional nanocrystal (NC) structures.[4–10] The purpose is not only to extend the optoelectronic functionalities by taking advantage of the quantum-confinement effect of organic-inorganic perovskites, but also to promote their potential applications in the emerging area of quantum information technologies. Single-particle optical studies of these organic-inorganic perovskite NCs, mainly in the forms of $MAPbX_3$ or $FAPbX_3$ ($MA^+ = CH_3NH_3^+$, $FA^+ = CH(NH_2)_2^+$, and $X^- = Br^-$ or I^-), are thus critical in revealing the intrinsic photophysical processes that are otherwise hidden from the ensemble-averaging measurements.[11,12] In the case of single $FAPbX_3$ NCs, the photoluminescence (PL) blinking behavior[13,14] and the single-photon emission feature[13–16] are now being routinely reported, with the additional demonstrations of the exciton-phonon coupling[16–18] and the crystal phase-transition[16,17] effects. Moreover, besides the extraction of charge-exciton and biexciton binding energies from single $FAPbX_3$ NCs,[18] they have also played a key role to demonstrate that the dark-exciton state is located lower in energy than those of the bright-exciton ones.[19]

In great contrast to the above $FAPbX_3$ NCs, the single $MAPbX_3$ NCs have received less research attention, especially in the quantum-optical studies, which is mainly caused by their structural and chemical instabilities promoting an irreversible process of light-induced degradation.[20–24] As such, the majority of the literature reports on single $MAPbX_3$ NCs are focused on the PL quenching/blinking[25–32] and the phase-transition characteristics,[33,34] the former of which is intimately related to the structural defects and the associated exciton charging or trapping events.[35,36] Despite recent advances in observing single-photon emission from single $MAPbX_3$ NCs on several occasions,[26,28] their exciton fine structures are yet to be revealed whose effective manipulations are currently one of

J. Yuan, C. Zhuang, Y. Zhou, C. Zhang, M. Xiao, X. Wang
School of Physics
National Laboratory of Solid State Microstructures
Collaborative Innovation Center of Advanced Microstructures
Nanjing University
Nanjing 210093, China
E-mail: mxiao@uark.edu; wxiaoyong@nju.edu.cn

D. Zhou, L. Wang
Key Laboratory of Flexible Electronics (KLOFE) & Institute of Advanced Materials (IAM)
Jiangsu National Synergetic Innovation Center for Advanced Materials (SICAM)
Nanjing Tech University (NanjingTech)
Nanjing 211816, China
E-mail: iamlwang@njtech.edu.cn

M. Xiao
Department of Physics
University of Arkansas
Fayetteville, AR 72701, USA

The ORCID identification number(s) for the author(s) of this article can be found under https://doi.org/10.1002/adom.202200606.

DOI: 10.1002/adom.202200606

the most exciting research topics covered by single all-inorganic $CsPbX_3$ and organic-inorganic $FAPbX_3$ NCs.[19,37–45] It is thus imperative to adopt new synthesis strategies or material structures for more robust investigations of single $MAPbX_3$ NCs, which are aimed not only to develop highly-efficient optoelectronic devices where their bulk materials have been studied the most,[1–3,46–48] but also to complement the well-studied $CsPbX_3$ and $FAPbX_3$ NCs for the joint advancement into quantum information technologies.

Here we have synthesized single $MAPbI_3$ microplates with the lateral dimension of several micrometers and the vertical thickness of tens of nanometers, and characterized their single-particle optical properties mainly at the cryogenic temperature. It is universal to see that multiple optical emitters are present in such a single $MAPbI_3$ microplate with the PL linewidths as narrow as ≈200 μeV, and they can behave like quantum-confined NCs with the single-photon emission feature. Due to the protection role played by the surrounding bulk material, the environmental charge fluctuations are effectively isolated from these single microplate $MAPbI_3$ NCs with the spectral diffusion effect being greatly suppressed. This allows us to reliably extract their exciton fine structures determined by the electron-hole exchange interaction, each of which is manifested as one set of doublet PL peaks with the orthogonally linear polarizations and a fine-structure splitting of ≈600 μeV. The above findings have thus demonstrated that the as-synthesized organic-inorganic microplates can serve as a potent platform to study the photophysical properties of single $MAPbI_3$ NCs, thus promising their potential applications in classical optoelectronic devices and quantum information technologies.

2. Results and Discussion

According to a two-step method as reported previously,[49,50] the single $MAPbI_3$ microplates are synthesized on top of a SiO_2/Si substrate by exposing solution-processed PbI_2 microplates to the MAI vapor in a chemical vapor deposition (CVD) system (see more details in the Experimental Section). As can be seen from the atomic force microscopy (AFM) image in **Figure 1**a, the lateral size and the vertical thickness of the as-synthesized single $MAPbI_3$ microplates are averaged at ≈1.1 μm and ≈51 nm, respectively. In Figure 1b, we present an optical image taken at one region of the sample substrate, wherein the single $MAPbI_3$ microplates are well separated from each other to facilitate the single-particle optical characterizations. To this end, the sample substrate is attached to the cold finger of a helium-free cryostat and the 640 nm (1.94 eV) output from a picosecond pulsed laser is focused to the spot size of ≈1 μm for the photoexcitation of a single $MAPbI_3$ microplate (see more details in the Experimental

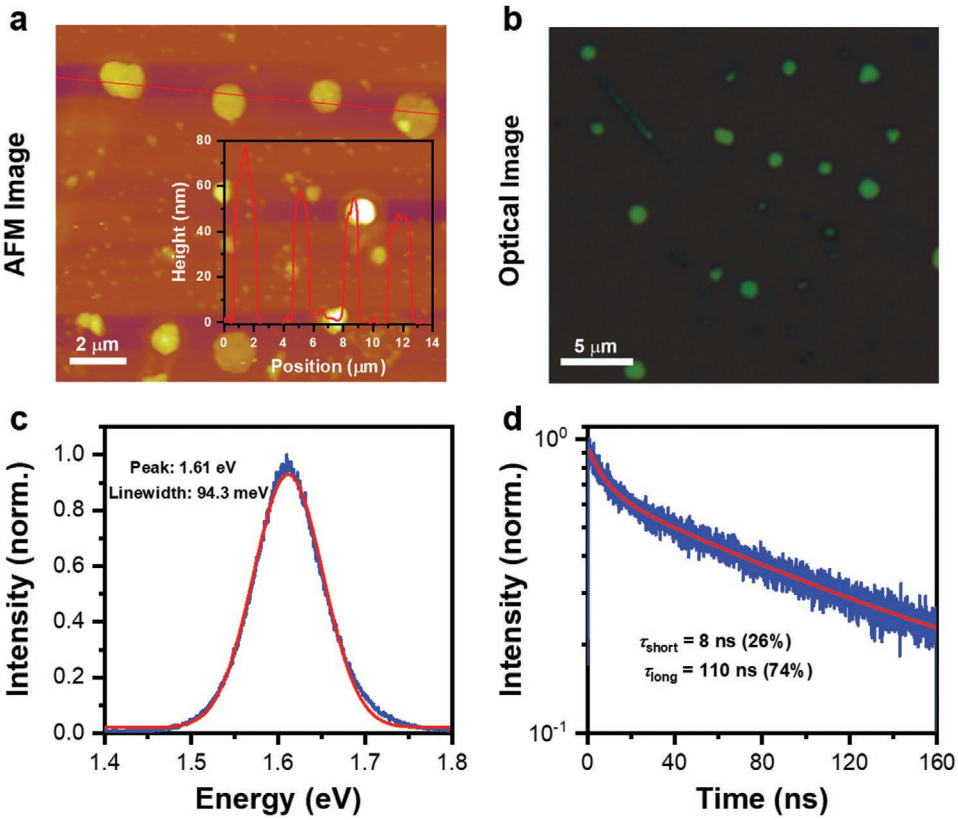

Figure 1. Room-temperature structural and optical characterizations of single $MAPbI_3$ microplates. a) AFM image of the sample substrate with a height profile measured across the solid red line being shown in the inset. b) Optical image of the sample substrate. c) PL spectrum (blue line) measured with an integration time of 1 s for a single $MAPbI_3$ microplate and fitted by a Gaussian function (red line). d) PL decay curve measured for this single $MAPbI_3$ microplate and fitted by a bi-exponential function with the short and long lifetimes of ≈8 ns (≈26%) and ≈110 ns (≈74%), respectively. In (c) and (d), the single $MAPbI_3$ microplate is excited at 640 nw with the laser power of ≈150 nW.

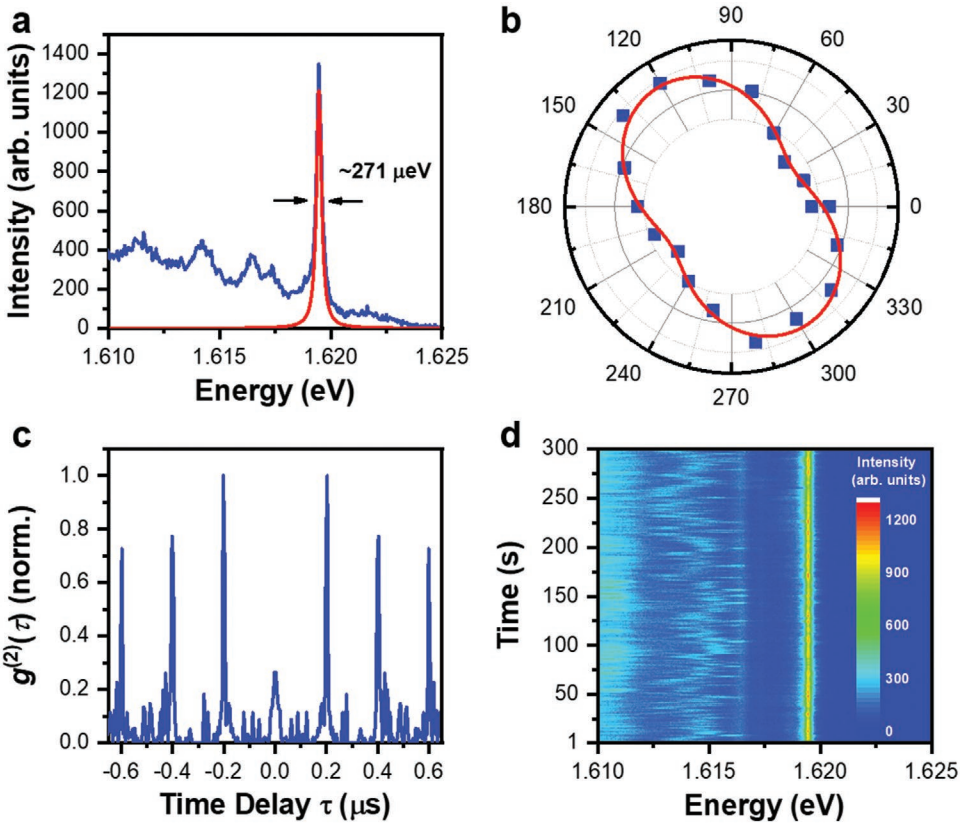

Figure 2. Optical characterizations of a single $MAPbI_3$ microplate at 4 K. a) PL spectrum (blue line) measured with the integration time of 1 s. The strong PL peak centered at ≈1.619 eV is fitted by a Lorentzian function with a linewidth of ≈271 ± 6.5 μeV. b) Polar plot showing intensity variation of this strong PL peak with the detection polarizer angle. c) Second-order photon correlation measurement of this strong PL peak with a $g^{(2)}(0)$ value of ≈0.26. To remove the background signal, this PL peak is spectrally filtered by a 1200 grooves per mm grating before entering the spectrometer exit slit. d) Time-dependent image constructed from 300 individual PL spectra measured for this single $MAPbI_3$ microplate. This single $MAPbI_3$ microplate is excited at 640 nm with a laser power of ≈150 nW.

Section). In Figure 1c, we plot the PL spectrum measured at room temperature for a representative single $MAPbI_3$ microplate, which is centered at ≈1.61 eV with a linewidth of ≈94.3 ± 0.2 meV. The PL decay curve measured for this single $MAPbI_3$ microplate is provided in Figure 1d, which can be fitted by a bi-exponential function with the short and long lifetimes of ≈8.0 ± 0.4 ns (≈26%) and ≈110.0 ± 4.9 ns (≈74%), respectively.

After room-temperature characterizations, we switch to the helium temperature of 4 K to explore how the PL spectrum of a single $MAPbI_3$ microplate would manifest itself under the reduced thermal influence. As shown in **Figure 2**a for a representative single $MAPbI_3$ microplate, on top of a broad background signal, a strong PL peak can be resolved at ≈1.619 eV together with several weak ones at its lower-energy side. The degree of linear polarization of this PL peak is estimated to be ≈35% from the polar plot shown in Figure 2b, where its intensity varies with the transmission angle of a linear polarizer placed in the PL collection path. It is further demonstrated in Figure 2c that this PL peak possesses the single-photon emission feature, with a $g^{(2)}(0)$ value of ≈0.26 being estimated from the second-order photon correlation measurement. As additionally shown in the Supporting Information, this kind of sharp PL peaks (Figure S1a,c, Supporting Information) with linear polarizations (Figure S1b,d, Supporting Information) and single-photon emissions (Figure S2a,b, Supporting Information) are commonly observed in 59 of the 71 single $MAPbI_3$ microplates studied in our experiment. For convenience, hereafter we will denote these sharp PL peaks as emanated from single microplate $MAPbI_3$ NCs due to their quantum-emitter feature. In a recent report on all-inorganic $CsPbBr_3$ microcrystals,[51] such single quantum emitters have also been discovered while the proposed origin of thickness variation and the associated formation of local energy minimum might also be applied to our current case.

The PL linewidth measured for the ≈1.619 eV peak in Figure 2a is ≈271 μeV and it can be as narrow as ≈200 μeV (see Figure S3, Supporting Information, for one example) among all the single $MAPbI_3$ NCs resolved by us from the studied microplates. Being on a par with those values associated with single all-inorganic $CsPbX_3$ NCs,[37–43] this PL linewidth is significantly smaller than what have ever been reported for single organic-inorganic $FAPbX_3$ ($FAPbI_3$: ≈0.8 meV[16]; $FAPbBr_3$: ≈0.4–3 meV[17–19]) or $MAPbX_3$ ($MAPbI_3$: ≈0.6 meV[33]; $MAPbBr_3$: ≈8 meV[34]) NCs at the cryogenic temperature. For the PL spectrum acquired with an integration time of 1 s in Figure 2a, its time evolution from 1 to 300 s is plotted in Figure 2d to reveal more clearly the coexistence of multiple single $MAPbI_3$ NCs and thus multiple energy minima localized in a single

microplate. A striking observation is that the PL spectra emitted by the two single microplate $MAPbI_3$ NCs at ≈1.619 and ≈1.616 eV are quite stable during the measurement time, while the other ones suffer strongly from the spectral diffusion effect. As has been well documented in the literature,[52–55] the MA^+ cations possess a higher polarity and a larger dipole moment than the Cs^+ and FA^+ anions, making the $MAPbX_3$ material more sensitive to the disturbance of local electric fields. Then the record-narrow PL linewidth measured here for single $MAPbI_3$ NCs, compared to those for single $FAPbX_3$ and $MAPbX_3$ NCs,[16–19,33,34] signifies the protection role played by the microplate in suppressing the spectral diffusion effect, which is normally caused by the surrounding charge fluctuations and the associated quantum-confined Stark effect.[56]

For the same single microplate $MAPbI_3$ NC studied in Figure 2, we next perform laser power- and temperature-dependent measurements to gain further insight into its photophysical properties. In **Figure 3**a, we plot the PL spectra measured at elevated laser powers from 100 to 180 nW. The integrated PL intensities (I) are shown in Figure 3b at different laser powers (P), which can be fitted by a power-law function of $I \propto P^{\alpha}$ with the exponent α of ≈0.96. This quasi-linear dependence of the PL intensity on laser power verifies that the optical emission should originate from exciton instead of trap-state recombination.[57,58] Still for this single microplate $MAPbI_3$ NC in Figure 3c, the PL spectrum is measured at increasing temperatures from 4 to 17 K, whose peak energy moves slightly to the blue side due to the dominance of lattice expansion over other bandgap shifting mechanisms.[53,58] When the sample temperature is further increased above 17 K, optical emission from this single microplate $MAPbI_3$ NC is completely quenched due to thermal activation of excitons from the local energy minimum to the surrounding bulk material.[51] The PL linewidth extracted from Figure 3c at each temperature is plotted in Figure 3d, which increases from ≈271 μeV at 4 K to ≈445 μeV at 15 K as a direct consequence of the enhanced exciton-phonon coupling.[16,17,33,34,53] This broadening of PL linewidth suggests that the optical emission of a single microplate $MAPbI_3$ NC is contributed by free excitons other than bound excitons, the latter of which should be temperature-insensitive owing to its lack of kinetic energy.[59] At the low temperatures below 20 K, the PL linewidth (Γ) broadening should be mainly contributed by the exciton-acoustic phonon coupling.[60] From the linear fit in Figure 3d using $\Gamma = \Gamma_0 + \gamma_{AC}T$, we can obtain Γ_0 = ≈172 μeV for the PL linewidth at 0 K and γ_{AC} = ≈22 μeV K^{-1} for the exciton-acoustic phonon

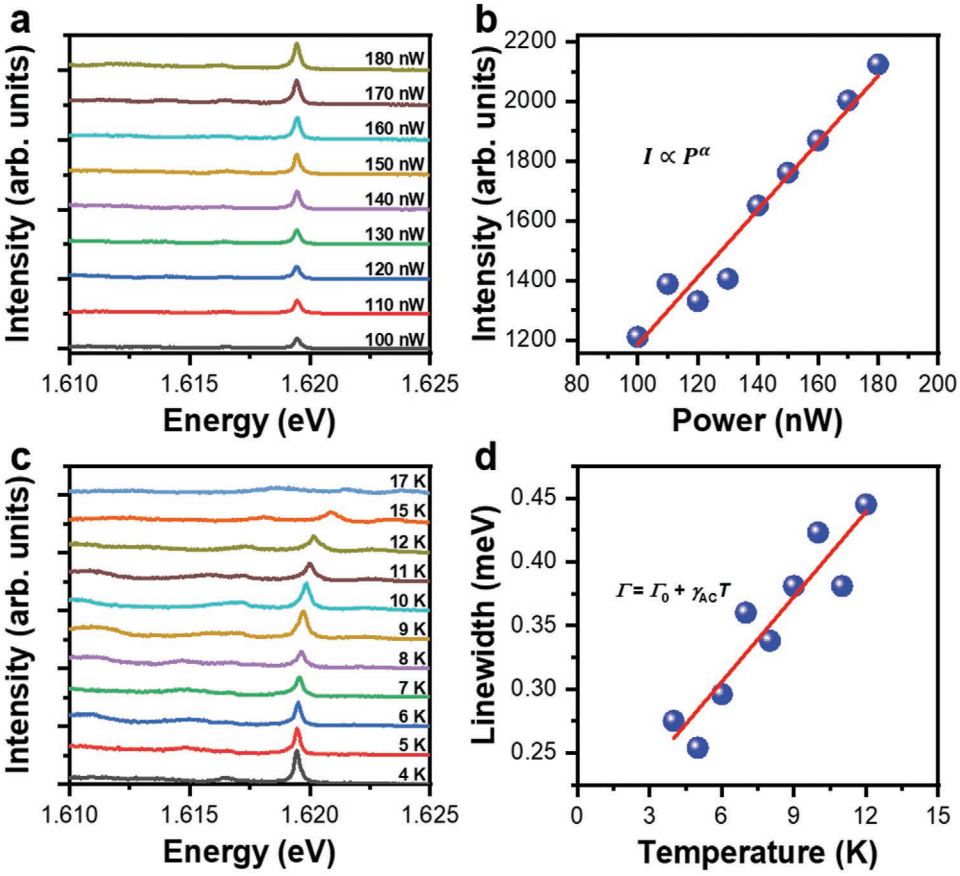

Figure 3. Laser power- and temperature-dependent optical properties of a single microplate $MAPbI_3$ NC. a) PL spectra measured at different laser powers at 4 K. b) Variation of the integrated PL intensity (I) with the laser power (P). The solid line is a power-law fitting of $I \propto P^{\alpha}$ with α = ≈0.96 ± 0.08. c) Temperature-dependent PL spectra measured at the laser power of 150 nW. d) PL linewidth (Γ) plotted as a function of the temperature (T) and fitted by the function form of $\Gamma = \Gamma_0 + \gamma_{AC}T$, with Γ_0 ≈ 172 ± 27.6 μeV and γ_{AC} ≈ 22 ± 3.3 μeV K^{-1}. This single microplate $MAPbI_3$ NC is excited at 640 nm, while the PL spectra in (a) and (c) are each acquired with an integration time of 1 s and offset to each other for clarity.

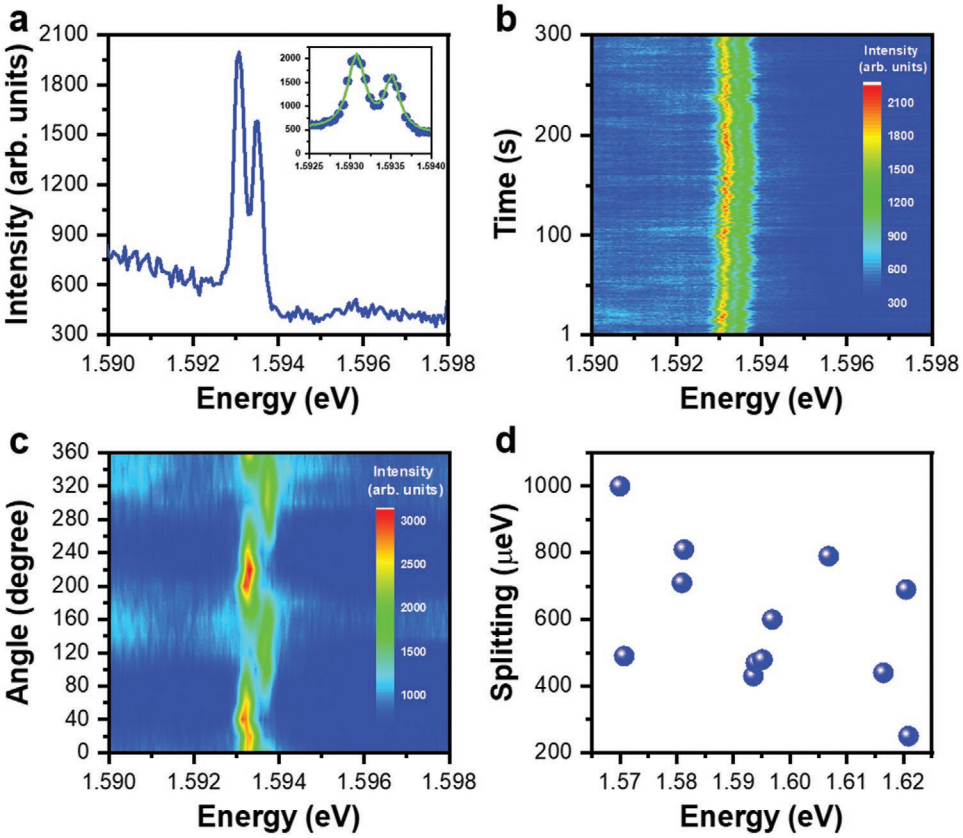

Figure 4. Exciton fine structures of single microplate $MAPbI_3$ NCs at 4 K. a) PL spectrum measured for a single microplate $MAPbI_3$ NC. Inset: enlarged view of the doublet peaks fitted by two Lorentzian functions. b) Time-dependent image of this single microplate $MAPbI_3$ NC constructed from 300 individual PL spectra. c) Polarization-dependent spectral image measured for this single microplate $MAPbI_3$ NC. d) Fine-structure splittings versus the emission energies for 12 single microplate $MAPbI_3$ NCs (see Table S1, Supporting Information, for the fitting errors of these fine-structure splittings). In (a)–(c), the single microplate $MAPbI_3$ NC is excited at 640 nm with a laser power of 150 nW, while each PL spectrum is acquired with an integration time of 1 s.

coupling coefficient. The exciton-acoustic phonon coupling of $MAPbI_3$ was normally ignored in previous optical studies of the bulk crystals[29,53] and the ensemble NCs,[61] while it was estimated to be ≈5 μeV K^{-1} for the single $FAPbI_3$ NCs,[16] ≈8 μeV K^{-1} for the single $CsPbBr_3$ NCs,[62] ≈8.9–23.9 μeV K^{-1} for the ensemble $CsPbBr_3$ NCs,[63] ≈60 μeV K^{-1} for the bulk $FAPbBr_3$ film,[60] and ≈60–78 μeV K^{-1} for the bulk $FAPbI_3$ film.[60,64]

In addition to the narrow single PL peak discussed above in Figures 2 and 3, the suppression of spectral diffusion has also allowed us to resolve the PL doublets, or exciton fine structures, from the remaining 12 of the total 71 single microplate $MAPbI_3$ NCs studied at 4 K. As shown in **Figure 4**a for a representative single microplate $MAPbI_3$ NC, one set of doublet PL peaks emerge from the background signal with the central emission energies of ≈1.5935 and ≈1.5931 eV, respectively. From the Lorentzian fittings in the inset of Figure 4a, the PL linewidths are estimated to be ≈208 and ≈274 μeV, respectively, for the high- and low-energy peaks of this PL doublet with a fine-structure splitting of ≈430 μeV. From the time-dependent spectral image plotted in Figure 4b, the high- and low-energy peaks suffer synchronously from a slight spectral diffusion effect, confirming their underlying origin from the same single microplate $MAPbI_3$ NC. Moreover, these doublet PL peaks have similar dependences on the laser power and sample temperature, as can be seen from Figure S4, Supporting Information. Most importantly, they possess orthogonally linear polarizations according to the anti-correlated intensity variations with the detection polarizer angles in Figure 4c, agreeing well with the same behavior demonstrated by fine-structured exciton states in single $CsPbX_3$ and $FAPbX_3$ NCs [19,37–40,43]

In Figure S5, Supporting Information, we have provided four more examples for the doublet PL peaks observed in single microplate $MAPbI_3$ NCs. The fine-structure splittings obtained for the total 11 single microplate $MAPbI_3$ NCs emitting PL doublets are plotted in Figure 4d versus their respective lower emission energies. The calculated average splitting of ≈597 ± 10.4 μeV is not significantly different from the value of ≈356 μeV previously reported for single $CsPbI_3$ NCs.[39] This is naturally expected since the conduction and valence bands of semiconductor perovskites are formed mainly by the Pb and I orbitals,[65,66] and the electron-hole exchange interaction giving rise to the exciton fine structure[19,38–40] should be little influenced by the MA^+, FA^+ or Cs^+ cation. This is further corroborated by the PL lifetime of ≈1 ns measured at 4 K for the single microplate $MAPbI_3$ NCs (see Figure S6, Supporting Information, for two examples), which is comparable to those values

reported for single $CsPbI_3$[39] and $FAPbI_3$[16] NCs to imply the similar strengths of exciton transition dipole moments.

3. Conclusion

To summarize, we have synthesized single $MAPbI_3$ microplates and discovered at the single-particle level that abundant optical emitters are present therein with the quantum feature of single-photon emission at the cryogenic temperature. Such novel quantum emitters, denoted by us as single microplate $MAPbI_3$ NCs, can possess a PL linewidth of ≈200 μeV that is the narrowest among all the currently-available values for single organic-inorganic perovskite NCs. This record-narrow PL linewidth is a direct consequence of the suppressed spectral diffusion effect, which has also allowed us for the first time to resolve the exciton fine structure from a single $MAPbI_3$ NC in the form of a PL doublet with the orthogonally linear polarizations and the energy separation of ≈600 μeV. The above findings in single microplate $MAPbI_3$ NCs, which are otherwise unachievable in their free-standing counterparts synthesized by traditional approaches, mark the successful addition of an important member into the family of low-dimensional perovskites carrying the quantum-optical and atomic-like characteristics required for quantum information technologies.

One unique structural anomaly of the $MAPbI_3$ material is that both the tetragonal and orthorhombic phases could coexist at the cryogenic temperature,[52,53,60,67–69] so that the single microplate NCs might originate from the small-sized tetragonal-like inclusions within the orthorhombic matrix. However, this possibility can be largely ruled out based on the temperature-dependent PL spectral measurements on single $MAPbI_3$ microplates (see Figure S7, Supporting Information, for one example), showing that their optical emission at 4 K is contributed exclusively by the orthorhombic phase. The temperature-dependent PL spectra shown in Figure S7, Supporting Information, also suggest that the single microplate NCs are not related to the trap-state emission due to the existence of impurities, since their emission energy should be hundreds of meV lower than that of the band-edge excitons.[69,70]

In analogy to the origin previously proposed for the single-photon emission from all-inorganic $CsPbBr_3$ microcrystals,[51] the single $MAPbI_3$ NCs observed here should be formed by thickness variation of the parent microplate. This kind of thickness variation is indeed observed on the surface of a single $MAPbI_3$ microplate, as can be seen from the SEM (scanning electron microscopy) and AFM images shown in Figures S8 and S9, Supporting Information, respectively. The photo-generated excitons would be trapped at local energy minima corresponding to different thicknesses, with the subsequent emission of multiple sharp PL peaks attached to a broad background spectrum from the remaining bulk material. In order to trigger the quantum-confinement effect, the vertical thickness or lateral size of a single microplate NC should be comparable to the bulk Bohr diameter of ≈4.4 nm.[71] As such, there exist more challenges and opportunities in future synthesis routes toward a full control over these structural parameters, aiming at the development of desired tunability and versatility for the newly-discovered single microplate $MAPbI_3$ NCs. Overall, we have demonstrated that the microplate host can render great optical stability to the embedded single $MAPbI_3$ NCs, which are equipped with superior photophysical and optoelectronic properties inherited from their bulk material. For example, the large absorption cross-section and the ease of being integrated into practical optoelectronic devices should be beneficial for the realization of ultrabright and electrically-pumped classical/quantum-optical light sources.

4. Experimental Section

Chemical Synthesis: The PbI_2 precursor solution was prepared by dissolving the PbI_2 powder in deionized water (1 mg mL^{-1}) at 90 °C under continuous stirring, and a small amount of it was drop-cast onto an oxygen-plasma-cleaned SiO_2/Si substrate, which was then heated from the room temperature to 180 °C within 5 min for the nucleation of PbI_2 microplates. The MAI powder was put in the upstream zone of a CVD tube heated at 115 °C for 100 min, and the evaporated MAI was transported at a flow rate of 50 sccm by a mixture of argon and hydrogen gases to the downstream zone. Therein, the MA^+ cations were successfully intercalated into the PbI_2 microplates on top of the SiO_2/Si substrate kept at 90 °C to yield the eventual formation of isolated $MAPbI_3$ microplates after 200 min.

Optical Characterization: The sample substrate containing single $MAPbI_3$ microplates was attached to the cold finger of a helium-free cryostat that could be operated at either room or cryogenic temperature. The output beam from a 640 nm picosecond diode laser operated at a repetition rate of 5 MHz was focused to a spot size of ≈1 μm onto the sample substrate by a dry objective with a numerical aperture of 0.82. The PL signal of a single $MAPbI_3$ microplate was collected by the same objective and sent through a 0.5 m spectrometer (with either 150 or 1200 grooves per mm grating) to a CCD camera for the PL spectral measurement. For the polarization-dependent measurement, a motorized half-wave plate would be rotated before a linear polarizer placed before the spectrometer, whose transmission axis was parallel to the grating grooves for maximizing the PL signal collected from a single $MAPbI_3$ microplate. After passing the spectrometer with a spectral resolution of ≈1 nm selected by the exit slit, the PL signal of a single $MAPbI_3$ microplate could be alternatively sent through a non-polarizing 50/50 beam splitter to two avalanche photodiodes (APDs) for the PL decay and second-order photon correlation measurements with a time resolution of ≈100 ps.

Supporting Information

Supporting Information is available from the Wiley Online Library or from the author.

Acknowledgements

J.Y. and D.Z. contributed equally to this work. This work is supported by the National Key Research and Development Program of China (No. 2019YFA0308700, No. 2021YFA1400803, and No. 2017YFA0303700), the National Natural Science Foundation of China (No. 62174081, No. 61974058 and No. 92064010), and the Priority Academic Program Development of Jiangsu Higher Education Institutions.

Conflict of Interest

The authors declare no conflict of interest.

Data Availability Statement

The data that support the findings of this study are available from the corresponding author upon reasonable request.

Keywords

$MAPbI_3$, microplates, nanocrystals, perovskites, single-photon emission

Received: March 15, 2022
Revised: May 4, 2022
Published online: June 25, 2022

[1] M. A. Green, A. Ho-Baillie, H. J. Snaith, *Nat. Photonics* **2014**, *8*, 506.
[2] X.-K. Liu, W. Xu, S. Bai, Y. Jin, J. Wang, R. H. Friend, F. Gao, *Nat. Mater.* **2021**, *20*, 10.
[3] S. D. Stranks, H. J. Snaith, *Nat. Nanotechnol.* **2015**, *10*, 391.
[4] F. Zhang, H. Zhong, C. Chen, X.-G. Wu, X. Hu, H. Huang, J. Han, B. Zou, Y. Dong, *ACS Nano* **2015**, *9*, 4533.
[5] H. Huang, A. S. Susha, S. V. Kershaw, T. F. Hung, A. L. Rogach, *Adv. Sci.* **2015**, *2*, 1500194.
[6] J. A. Sichert, Y. Tong, N. Mutz, M. Vollmer, S. Fischer, K. Z. Milowska, R. G. Cortadella, B. Nickel, C. Cardenas-Daw, J. K. Stolarczyk, A. S. Urban, J. Feldmann, *Nano Lett.* **2015**, *15*, 6521.
[7] D. Di, K. P. Musselman, G. Li, A. Sadhanala, Y. Ievskaya, Q. Song, Z. K. Tan, M. L. Lai, J. L. MacManus-Driscoll, N. C. Greenham, R. H. Friend, *J. Phys. Chem. Lett.* **2015**, *6*, 446.
[8] L. Protesescu, S. Yakunin, M. I. Bodnarchuk, F. Bertolotti, N. Masciocchi, A. Guagliardi, M. V. Kovalenko, *J. Am. Chem. Soc.* **2016**, *138*, 14202.
[9] L. Protesescu, S. Yakunin, S. Kumar, J. Bär, F. Bertolotti, N. Masciocchi, A. Guagliardi, M. Grotevent, I. Shorubalko, M. I. Bodnarchuk, C.-J. Shih, M. V. Kovalenko, *ACS Nano* **2017**, *11*, 3119.
[10] I. Levchuk, A. Osvet, X. Tang, M. Brandl, J. D. Perea, F. Hoegl, G. J. Matt, R. Hock, M. Batentschuk, C. J. Brabec, *Nano Lett.* **2017**, *17*, 2765.
[11] Z. Cao, F. Hu, C. Zhang, S. N. Zhu, M. Xiao, X. Wang, *Adv. Photonics* **2020**, *2*, 054001.
[12] L. Hou, P. Tamarat, B. Lounis, *Nanomaterials* **2021**, *11*, 1058.
[13] N. Yarita, H. Tahara, M. Saruyama, T. Kawawaki, R. Sato, T. Teranishi, Y. Kanemitsu, *J. Phys. Chem. Lett.* **2017**, *8*, 6041.
[14] C. T. Trinh, D. N. Minh, K. J. Ahn, Y. Kang, K.-G. Lee, *ACS Photonics* **2018**, *5*, 4937.
[15] J. Liu, F. Hu, Y. Zhou, C. Zhang, X. Wang, M. Xiao, *J. Lumin.* **2020**, *221*, 117032.
[16] M. Fu, P. Tamarat, J.-B. Trebbia, M. I. Bodnarchuk, M. V. Kovalenko, J. Even, B. Lounis, *Nat. Commun.* **2018**, *9*, 3318.
[17] O. Pfingsten, J. Klein, L. Protesescu, M. I. Bodnarchuk, M. V. Kovalenko, G. Bacher, *Nano Lett.* **2018**, *18*, 4440.
[18] K. Cho, T. Yamada, H. Tahara, T. Tadano, H. Suzuura, M. Saruyama, R. Sato, T. Teranishi, Y. Kanemitsu, *Nano Lett.* **2021**, *21*, 7206.
[19] P. Tamarat, M. I. Bodnarchuk, J.-B. Trebbia, R. Erni, M. V. Kovalenko, J. Even, B. Lounis, *Nat. Mater.* **2019**, *18*, 717.
[20] G. Niu, W. Li, F. Meng, L. Wang, H. Dong, Y. Qiu, *J. Mater. Chem. A* **2014**, *2*, 705.
[21] B. Conings, J. Drijkoningen, N. Gauquelin, A. Babayigit, J. D'Haen, L. D'Olieslaeger, A. Ethirajan, J. Verbeeck, J. Manca, E. Mosconi, F. D. Angelis, H.-G. Boyen, *Adv. Energy Mater.* **2015**, *5*, 1500477.
[22] L. Zhang, P. H.-L. Sit, *J. Phys. Chem. C* **2015**, *119*, 22370.
[23] N. Aristidou, I. Sanchez-Molina, T. Chotchuangchutchaval, M. Brown, L. Martinez, T. Rath, S. A. Haque, *Angew. Chem., Int. Ed.* **2015**, *54*, 8208.
[24] E. J. Juarez-Perez, Z. Hawash, S. R. Raga, L. K. Ono, Y. Qi, *Energy Environ. Sci.* **2016**, *9*, 3406.
[25] J. F. Galisteo-López, M. E. Calvo, T. C. Rojas, H. Míguez, *ACS Appl. Mater. Interfaces* **2019**, *11*, 6344.
[26] L. Chouhan, S. Ito, E. M. Thomas, Y. Takano, S. Ghimire, H. Miyasaka, V. Biju, *ACS Nano* **2021**, *15*, 2831.
[27] L. Liu, L. Deng, S. Huang, P. Zhang, J. Linnros, H. Zhong, I. Sychugov, *J. Phys. Chem. Lett.* **2019**, *10*, 864.
[28] X. Han, G. Zhang, B. Li, C. Yang, W. Guo, X. Bai, P. Huang, R. Chen, C. Qin, J. Hu, Y. Ma, H. Zhong, L. Xiao, S. Jia, *Small* **2020**, *16*, 2005435.
[29] B. Yin, J. Cavin, D. Wang, D. Khan, M. Shen, C. Laing, R. Mishra, B. Sadtler, *J. Mater. Chem. C* **2019**, *7*, 3486.
[30] T. Kim, S. I. Jung, S. Ham, H. Chung, D. Kim, *Small* **2019**, *15*, 1900355.
[31] Y. Kimura, I. Karimata, Y. Kobori, T. Tachikawa, *ChemNanoMat* **2019**, *5*, 340.
[32] L. Chouhan, S. Ghimire, V. Biju, *Angew. Chem., Int. Ed.* **2019**, *58*, 4875.
[33] L. Liu, F. Pevere, F. Zhang, H. Zhong, I. Sychugov, *Phys. Rev. B* **2019**, *100*, 195430.
[34] L. Liu, R. Zhao, C. Xiao, F. Zhang, F. Pevere, K. Shi, H. Huang, H. Zhong, I. Sychugov, *J. Phys. Chem. Lett.* **2019**, *10*, 5451.
[35] X. Wen, A. Ho-Baillie, S. Huang, R. Sheng, S. Chen, H.-C. Ko, M. A. Green, *Nano Lett.* **2015**, *15*, 4644.
[36] Y. Tian, A. Merdasa, M. Peter, M. Abdellah, K. Zheng, C. S. Ponseca Jr., T. Pullerits, A. Yartsev, V. Sundström, I. G. Scheblykin, *Nano Lett.* **2015**, *15*, 1603.
[37] G. Rainò, G. Nedelcu, L. Protesescu, M. I. Bodnarchuk, M. V. Kovalenko, R. F. Mahrt, T. Stöferle, *ACS Nano* **2016**, *10*, 2485.
[38] M. Fu, P. Tamarat, H. Huang, J. Even, A. L. Rogach, B. Lounis, *Nano Lett.* **2017**, *17*, 2895.
[39] C. Yin, L. Chen, N. Song, Y. Lv, F. Hu, C. Sun, W. W. Yu, C. Zhang, X. Wang, Y. Zhang, M. Xiao, *Phys. Rev. Lett.* **2017**, *119*, 026401.
[40] M. A. Becker, R. Vaxenburg, G. Nedelcu, P. C. Sercel, A. Shabaev, M. J. Mehl, J. G. Michopoulos, S. G. Lambrakos, N. Bernstein, J. L. Lyons, T. Stöferle, R. F. Mahrt, M. V. Kovalenko, D. J. Norris, G. Rainò, A. L. Efros, *Nature* **2018**, *553*, 189.
[41] H. Utzat, W. Sun, A. E. K. Kaplan, F. Krieg, M. Ginterseder, B. Spokoyny, N. D. Klein, K. E. Shulenberger, C. F. Perkinson, M. V. Kovalenko, M. G. Bawendi, *Science* **2019**, *363*, 1068.
[42] Y. Lv, C. Yin, C. Zhang, W. W. Yu, X. Wang, Y. Zhang, M. Xiao, *Nano Lett.* **2019**, *19*, 4442.
[43] P. Tamarat, L. Hou, J.-B. Trebbia, A. Swarnkar, L. Biadala, Y. Louyer, M. I. Bodnarchuk, M. V. Kovalenko, J. Even, B. Lounis, *Nat. Commun.* **2020**, *11*, 6001.
[44] Y. Lv, C. Yin, C. Zhang, X. Wang, Z.-G. Yu, M. Xiao, *Nat. Commun.* **2021**, *12*, 2192.
[45] B. Lv, T. Zhu, Y. Tang, Y. Lv, C. Zhang, X. Wang, D. Shu, M. Xiao, *Phys. Rev. Lett.* **2021**, *126*, 197403.
[46] H. Zhou, Q. Chen, G. Li, S. Luo, T.-B. Song, H.-S. Duan, Z. Hong, J. You, Y. Liu, Y. Yang, *Science* **2014**, *345*, 542.
[47] Z. K. Tan, R. S. Moghaddam, M. L. Lai, P. Docampo, R. Higler, F. Deschler, M. Price, A. Sadhanala, L. M. Pazos, D. Credgington, F. Hanusch, T. Bein, H. J. Snaith, R. H. Friend, *Nat. Nanotechnol.* **2014**, *9*, 687.
[48] G. Xing, N. Mathews, S. S. Lim, N. Yantara, X. Liu, D. Sabba, M. Grätzel, S. Mhaisalkar, T. C. Sum, *Nat. Mater.* **2014**, *13*, 476.
[49] Y. Sun, Z. Zhou, Z. Huang, J. Wu, L. Zhou, Y. Cheng, J. Liu, C. Zhu, M. Yu, P. Yu, W. Zhu, Y. Liu, J. Zhou, B. Liu, H. Xie, Y. Cao, H. Li, X. Wang, K. Liu, X. Wang, J. Wang, L. Wang, W. Huang, *Adv. Mater.* **2019**, *31*, 1806562.
[50] Y. Sun, Y. Yin, M. Pols, J. Zhong, Z. Huang, B. Liu, J. Liu, W. Wang, H. Xie, G. Zhan, Z. Zhou, W. Zhang, P. Wang, C. Zha, X. Jiang,

Y. Ruan, C. Zhu, G. Brocks, X. Wang, L. Wang, J. Wang, S. Tao, W. Huang, *Adv. Mater.* **2020**, *32*, 2002392.
[51] S. Feng, Q. Qin, X. Han, C. Zhang, X. Wang, T. Yu, M. Xiao, *Adv. Mater.* **2022**, *34*, 2106278.
[52] J. M. Frost, K. T. Butler, F. Brivio, C. H. Hendon, M. van Schilfgaarde, A. Walsh, *Nano Lett.* **2014**, *14*, 2584.
[53] M. I. Dar, G. Jacopin, S. Meloni, A. Mattoni, N. Arora, A. Boziki, S. M. Zakeeruddin, U. Rothlisberger, M. Grätzel, *Sci. Adv.* **2016**, *2*, e1601156.
[54] G. Walters, M. Wei, O. Voznyy, R. Quintero-Bermudez, A. Kiani, D. M. Smilgies, R. Munir, A. Amassian, S. Hoogland, E. Sargent, *Nat. Commun.* **2018**, *9*, 4214.
[55] S. Ham, H. Chung, T.-W. Kim, J. Kim, D. Kim, *Nanoscale* **2018**, *10*, 2207.
[56] S. A. Empedocles, M. G. Bawendi, *Science* **1997**, *278*, 2114.
[57] T. Schmidt, K. Lischka, W. Zulehner, *Phys. Rev. B* **1992**, *45*, 8989.
[58] H. H. Fang, R. Raissa, M. Abdu-Aguye, S. Adjokatse, G. R. Blake, J. Even, M. A. Loi, *Adv. Funct. Mater.* **2015**, *25*, 2378.
[59] Y. Pelant, J. Valanta, *Luminescence Spectroscopy of Semiconductors*, Oxford University Press, Oxford, UK **2012**.
[60] A. D. Wright, C. Verdi, R. L. Milot, G. E. Eperon, M. A. Pérez-Osorio, H. J. Snaith, F. Giustino, M. B. Johnston, L. M. Herz, *Nat. Commun.* **2016**, *7*, 11755.
[61] Z.-F. Shi, Y. Li, S. Li, H.-F. Ji, L.-Z. Lei, D. Wu, T.-T. Xu, J.-M. Xu, Y.-T. Tian, X.-J. Li, *J. Mater. Chem. C* **2017**, *5*, 8699.
[62] J. Ramade, L. M. Andriambariarijaona, V. Steinmetz, N. Goubet, L. Legrand, T. Barisien, F. Bernardot, C. Testelin, E. Lhuillier, A. Bramati, M. Chamarro, *Appl. Phys. Lett.* **2018**, *112*, 072104.
[63] A. Shinde, R. Gahlaut, S. Mahamuni, *J. Phys. Chem. C* **2017**, *121*, 14872.
[64] H.-H. Fang, F. Wang, S. Adjokatse, N. Zhao, J. Even, M. A. Loi, *Light: Sci. Appl.* **2015**, *5*, e16056.
[65] I. Borriello, G. Cantele, D. Ninno, *Phys. Rev. B* **2008**, *77*, 235214.
[66] F. Brivio, A. B. Walker, A. Walsh, *APL Mater.* **2013**, *1*, 042111.
[67] C. Wehrenfennig, M. Liu, H. J. Snaith, M. B. Johnston, L. M. Herz, *APL Mater.* **2014**, *2*, 081513.
[68] D. Li, G. Wang, H.-C. Cheng, C.-Y. Chen, H. Wu, Y. Liu, Y. Huang, X. Duan, *Nat. Commun.* **2016**, *7*, 11330.
[69] L. Q. Phuong, Y. Yamada, M. Nagai, N. Maruyama, A. Wakamiya, Y. Kanemitsu, *J. Phys. Chem. Lett.* **2016**, *7*, 2316.
[70] X. Wu, M. T. Trinh, D. Niesner, H. Zhu, Z. Norman, J. S. Owen, O. Yaffe, B. J. Kudisch, X.-Y. Zhu, *J. Am. Chem. Soc.* **2015**, *137*, 2089.
[71] K. Tanaka, T. Takahashi, T. Ban, T. Kondo, K. Uchida, N. Miura, *Solid State Commun.* **2003**, *127*, 619.